Investigation of magnetic anisotropy and magnetization reversal by planar Hall effect in Fe_3Si and Fe films grown on GaAs(113)A substrates

2006 J. Phys.: Condens. Matter 18 9453

(http://iopscience.iop.org/0953-8984/18/41/012)

INSTITUTE OF PHYSICS PUBLISHING JOURNAL OF PHYSICS: CONDENSED MATTER

J. Phys.: Condens. Matter **18** (2006) 9453–9462 doi:10.1088/0953-8984/18/41/012

Investigation of magnetic anisotropy and magnetization reversal by planar Hall effect in Fe_3Si and Fe films grown on GaAs(113)A substrates

P K Muduli[1], K-J Friedland, J Herfort, H-P Schönherr and K H Ploog

Paul-Drude-Institut für Festkörperelektronik, Hausvogteiplatz 5-7, D-10117 Berlin, Germany

E-mail: pranabmuduli@gmail.com

Received 1 August 2006, in final form 12 September 2006
Published 29 September 2006
Online at stacks.iop.org/JPhysCM/18/9453

Abstract

Magnetic anisotropy and magnetization reversal in Fe_3Si and Fe films grown on GaAs(113)A substrates are studied using the planar Hall effect (PHE). The PHE in this orientation exhibits an antisymmetric component in addition to the usual symmetric component. The relative magnitude of symmetric and antisymmetric components in the PHE is affected by the composition of the Fe_3Si films and the thickness of the Fe films, which lead to a complex behaviour of the planar Hall resistivity in the low magnetic field region below saturation. However, irrespective of the composition/thickness of the films, magnetization reversal can be described qualitatively within a single domain by the simple Stoner–Wolfarth model of magnetization reversal. This allows us to determine the magnetic anisotropy properties of these films in good agreement with the experimental results of anisotropic magnetoresistance and superconducting quantum interference device magnetometry.

(Some figures in this article are in colour only in the electronic version)

1. Introduction

An understanding of the magnetic anisotropy in epitaxial films is crucial to engineer the magnetic properties. Recently, the planar Hall effect (PHE) has emerged as a popular tool for studying magnetic anisotropy and magnetization reversal in ferromagnetic thin films grown on semiconducting substrates [1–4], which are promising for spintronics applications. PHE refers to the resulting electric field developed perpendicular to the current direction and which lies in the plane of the current and magnetic field. In fact, PHE and other magnetotransport effects, such as anisotropic magnetoresistance and the anomalous Hall effect, are very sensitive tools for studying magnetic anisotropy and magnetization reversal in these low-dimensional magnetic

[1] Present address: Department of Physics and Astronomy, University of North Carolina, Chapel Hill, NC 27599-3255, USA.

structures, particularly because of their relative insensitivity to the semiconducting or insulating substrate. For thin films, it is difficult to subtract the magnetic contribution of the substrate in traditional magnetometry techniques like vibrating sample magnetometry or superconducting quantum interference device (SQUID) magnetometry. In magnetotransport measurements, only the metallic portion (or the film portion) of the sample is measured. In our previous works, we reported these magnetotransport effects from epitaxial Fe [5, 3] and Fe_3Si [6] films on a high-index substrate, namely GaAs(113)A. The unique orientation used in these studies has a low surface symmetry and results in an additional antisymmetric component in the PHE [6]. The antisymmetric component manifests itself as a change in sign of the PHE when the direction of the in-plane applied saturated magnetic field is reversed, and is a unique observation of a second-order Hall effect. In [6], the behaviour of PHE for Fe_3Si on GaAs(113)A was discussed as a function of composition and temperature. However, the discussion was restricted to high magnetic fields above saturation. In this paper we will concentrate on the low magnetic field behaviour of PHE below saturation and use it to determine the magnetic anisotropy of these high-index orientation films. We will discuss the magnetization reversal in the Fe_3Si films over a range of compositions and also extend the study to Fe films of different thicknesses. The room-temperature values of the phenomenological coefficients of the PHE and their behaviour with composition of Fe_3Si and thickness of Fe films will also be discussed. It should be mentioned that both Fe and Fe_3Si are ferromagnetic at room temperature and have a close lattice match with GaAs. Thus, these are highly promising material systems for spintronics applications.

2. Experiment

The high-quality Fe_3Si and Fe films used in this work were grown on GaAs(113)A substrates by molecular-beam epitaxy [7, 8]. Fe_3Si films were grown at a growth temperature of 250 °C, whereas the Fe films were grown at a relatively low growth temperature of 0 °C. Films grown under these conditions exhibit a high crystal quality and a smooth interface/surface, keeping the same orientation of the substrate. The phase boundary of the stable Fe_3Si phase covers a range from 9 to 26.6 at.% Si [9, 10]. This offers the advantage of varying the composition, and hence the magnetic properties in these films, while maintaining the cubic crystal structure. In [7], we demonstrated the growth and stability of $Fe_{3+x}Si_{1-x}$ films on GaAs(113)A substrates over a range of compositions of $0.4 > x > -0.06$, where x denotes the deviation from stoichiometry. These high-quality films are used in the present study of the PHE. For the PHE measurements, the layers were lithographically patterned into Hall bars 30 μm in width and with a 22.5 μm separation between the voltage leads for electrical transport measurements. The behaviour of the PHE for two different kinds of measurements will be discussed. First, the in-plane field orientation is kept fixed along a specific direction with respect to the longitudinal axis of the Hall bars, while the field magnitude is swept linearly. Second, we studied the angular dependence of the PHE response when a fixed in-plane magnetic field was applied. As the low transverse Hall resistivity, ρ_{xy}, is smaller than the longitudinal resistivity, ρ_{xx}, some crossover from ρ_{xx} to ρ_{xy} may appear. In this case, we have corrected ρ_{xy} by $\rho_{xy}^{\mathrm{corr}}(H, \theta_{\mathrm{H}}) = \rho_{xy}(H, \theta_{\mathrm{H}}) - \gamma\, \rho_{xx}(H, \theta_{\mathrm{H}})$, where the factor γ was kept constant for a particular contact configuration. All measurements shown in this work will be restricted to room temperature for simplicity.

3. Results

In figure 1, we show the magnetic field dependence of planar Hall resistivity ρ_{xy} in $Fe_{3+x}Si_{1-x}$ films grown on GaAs(113)A substrates for two different compositions, $x = 0.15$ and 0.07. The

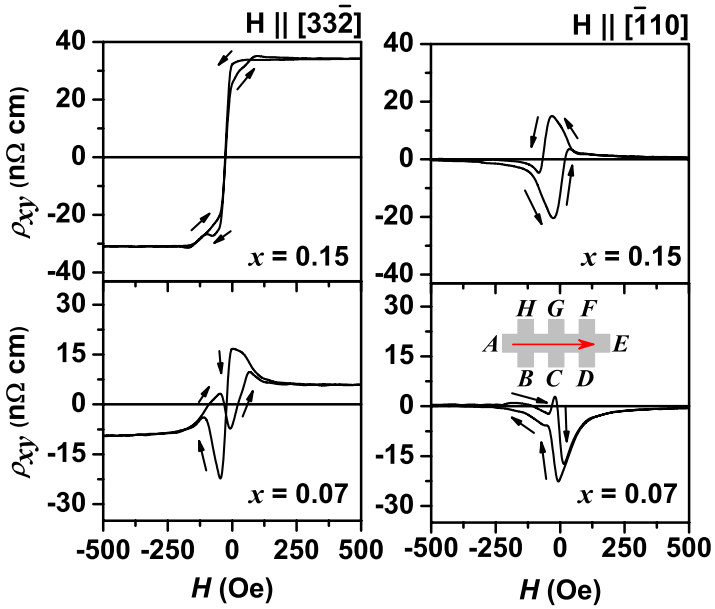

Figure 1. Field dependence of the PHE (ρ_{xy}) from $Fe_{3+x}Si_{1-x}$(113) films at 300 K. The first (second) column is for a magnetic field applied parallel to the major in-plane [33$\bar{2}$] ([$\bar{1}$10]) axis, whereas the first (second) row is for a $Fe_{3+x}Si_{1-x}$ layer with $x = 0.15$ ($x = 0.07$). The inset on the lower right plot shows a schematic of the contacts and geometry of the PHE measurements, with the arrow showing the current direction along [33$\bar{2}$].

planar Hall resistivities are shown for a magnetic field parallel to the two major in-plane [33$\bar{2}$] and [$\bar{1}$10] axes, which are perpendicular to each other. The measurement geometry is similar to [6]. The current was applied along the contacts AE and the PHE (ρ_{xy}) was measured along the contacts such as BH in a counterclockwise sense, as shown in the inset of figure 1. The current direction was made parallel to the [33$\bar{2}$] direction so that the PHE is measured along the [$\bar{1}$10] direction. The characteristic properties of ρ_{xy} in this figure can be understood from the following equation developed in [6] for [113]-oriented films:

$$\rho_{xy} = \rho_s^{\mathrm{PHE}} \sin 2\theta_M + \rho_{\mathrm{SATM}}^0 \cos\theta_M + \rho_{\mathrm{SATM}}^1 \cos^3\theta_M, \tag{1}$$

where $\rho_s^{\mathrm{PHE}} = (9C_1 + 2C_4)/22$, $\rho_{\mathrm{SATM}}^0 = 9(a_{12223} - a_{11123})/(11\sqrt{2})$, and $\rho_{\mathrm{SATM}}^1 = -42\sqrt{2}(a_{12223} - a_{11123})/121$. Here, the coefficients C_1 and C_4 relate to the symmetric component of the magnetoresistivity tensor, whereas the coefficients a_{12223} and a_{11123} relate to the antisymmetric component of the magnetoresistivity tensor. θ_M represents the direction of magnetization **M** with respect to the [33$\bar{2}$] direction. Let θ_H represents the applied magnetic field **H** with respect to the [33$\bar{2}$] direction. When a saturating field is applied along [33$\bar{2}$] (which represents a low-symmetry axis), $\theta_H = \theta_M = 0$, and the PHE in figure 1 exhibits a sign change when the direction of the applied field is reversed. Clearly, this is associated with the last two terms in equation (1), which originate from the antisymmetric component of the magnetorestivity tensors and are non-zero along this axis. When the saturating magnetic field is applied along [$\bar{1}$10], $\theta_H = \theta_M = 90^\circ$ and hence the antisymmetric components involving cosine terms vanish. In this case, the PHE is an even function of the applied magnetic field. In other words, only the first term in equation (1), which arises from the symmetric component of the magnetoresistivity tensor, contributes.

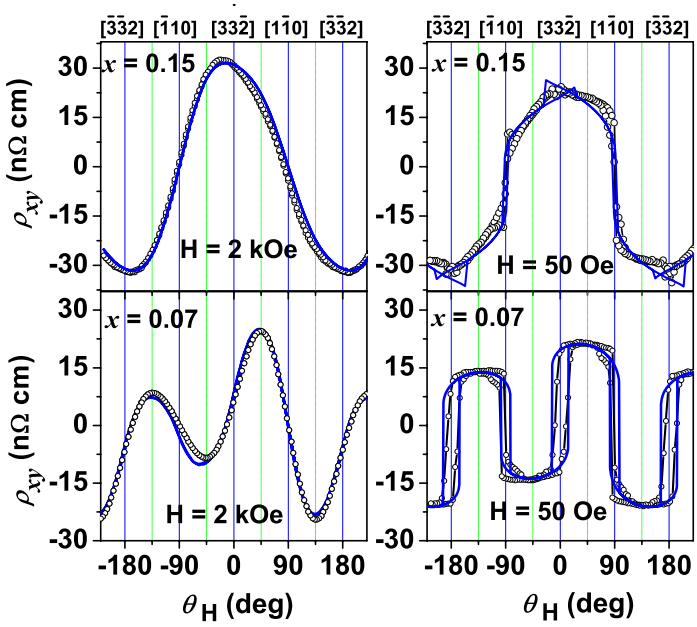

Figure 2. Experimental (symbols) and calculated (thick solid line) angular dependences of PHE (ρ_{xy}) for two $Fe_{3+x}Si_{1-x}$ samples with $x = 0.15$ (first row) and $x = 0.07$ (second row) at applied field strengths of $H = +2$ kOe (first column) and $H = +50$ Oe (second column). Here, $\theta_H = 0°$ corresponds to the $[33\bar{2}]$ direction, which is also the direction of the current.

At low magnetic field below saturation, the behaviour of the planar Hall resistivity for the two samples along the two directions differ significantly. In fact, at low magnetic field the magnetization is not saturated and hence $\theta_H \neq \theta_M$. Thus, the behaviour of the PHE is sensitive to the manner in which the magnetization rotates in-plane, which in turn is sensitive to the magnetic anisotropy and the mechanism of magnetization reversal. This is the focus of this paper. In figure 1, the arrows in the low magnetic field show the behaviour of the PHE as the direction of the field is reversed. Clearly, the behaviour is very different in both directions as well as for both samples. This seems to indicate a very different mechanism of magnetization reversal in all these cases. However, we will show that the resulting different behaviour is a consequence of the presence of an antisymmetric component which changes with the direction of the applied magnetic field and the composition of the films, and that the mechanism of the rotation of magnetization is similar in all these cases.

In order to completely understand the behaviour of the PHE in figure 1, first we calculate the amplitudes of the PHE in equation (1), namely ρ_s^{PHE}, ρ_{SATM}^0, and ρ_{SATM}^1 by using the high-field angular dependence of the PHE. The angular dependence of ρ_{xy} is shown in figure 2 at different applied magnetic fields. At high magnetic field, e.g. for $H = +2$ kOe, the magnetization is completely saturated and the PHE is completely reversible. From the fitting of this high-field behaviour (shown as a solid line) with equation (1), we determine the PHE amplitudes ρ_s^{PHE}, ρ_{SATM}^0, and ρ_{SATM}^1. By lowering the magnetic field, the magnetization deviates from the one imposed by the external magnetic field and ρ_{xy} exhibit jumps with hysteresis behaviour. The four-jumps in the low-field behaviour from 0° to 360° are interpreted as four hard axes, in other words the presence of a four-fold magnetic anisotropy [3]. However, the amplitude of the jumps as well as the width of the jumps along 0° (180°) is very different

compared to that along 90° (−90°). To understand these rather unusual PHE response curves in detail, we model the magnetic anisotropy of these films. It is known that the Fe films grown on GaAs(113)A substrates exhibit a combination of four-fold and a uniaxial magnetic anisotropy (UMA) [8, 11]. Since Fe_3Si also has a cubic structure, we consider a similar magnetic anisotropy for both systems. The in-plane magnetic anisotropy energy density, E_{IPMA}, for (113) surface symmetry can be obtained by using the symmetry of the (113) surface and taking into account the large demagnetization energy of these films, similarly to Fe/GaAs(113)A films [8]:

$$E_{\mathrm{IPMA}} = (K_1/484)[89 + 16\cos 2\theta_{\mathrm{M}} + 48\cos 4\theta_{\mathrm{M}}] + K_{\mathrm{u}}\sin^2(\theta_{\mathrm{M}}) - MH\cos\theta_{\mathrm{H}} \tag{2}$$

where K_1 and K_{u} are the cubic four-fold and uniaxial anisotropy constants, respectively. The magnetization **M** is assumed to lie in-plane, which is justified given the large demagnetization energy of these films. The first two terms in the above equation involving K_1 and K_{u} represent the four-fold and uniaxial magnetic anisotropy, respectively, whereas the last term represents the Zeeman energy. Using this anisotropy energy, we calculate the low-field PHE response of figures 1 and 2. The hysteresis behaviour of the sample is modelled using a single-domain model [12–15], where the magnetization is assumed to rotate coherently according to the Stoner–Wohlfarth (SW) model [16]. In this model, the magnetic anisotropy energy E_{IPMA} and the history of the applied field **H** determine the orientation of **M**, which changes the angle θ_{M} while maintaining the saturation magnitude M_{s}. At high field, **M** lies in a global minimum of E_{IPMA} at χ (H, θ_{H}). As the direction/magnitude of **H** is changed, **M** rotates to follow the locus of this energy minimum χ (H, θ_{H}). Magnetic switching occurs at the point where this minimum vanishes, when **M** jumps to the new neighbouring minimum. It is possible to determine wether the jumps observed in the data of figures 1 and 2 are determined by the SW model or not. In order to do this, we calculate the PHE response using the SW model. First, the angle of magnetization was derived by numerically tracking the evolution of the local minimum of the free energy in equation (2), and then equation (1) is used to find the PHE response. The final calculated PHE response curves are shown in the low-field behaviour of figure 2 as solid lines. We use K_1/M_{s} and the uniaxial ratio, $r = K_{\mathrm{u}}/K_1$, as fitting parameters. As can be seen, there is a very good qualitative agreement between the calculated and experimental curves. The amplitude and the width of the jumps in the PHE at 0° (180°) and 90° (−90°) are correctly reproduced. In fact, the larger width of the jumps in PHE at 0° compared to 90° imply that the $[33\bar{2}]$ axis, which represents 0°, is harder compared to the $[\bar{1}10]$ axis, indicating the presence of a UMA with an easy axis along $[\bar{1}10]$. At very low field, the calculated planar Hall resistivity deviates slightly from the experimental curve, since at such low field the rotation of magnetization is solely determined by the microscopic magnetic structure of the sample. This is the reason why the irreversible part does not agree with the SW model.

The field dependence of the PHE can also be calculated in a similar manner. In this case, we numerically track the minima in anisotropy energy as the field is swept and then use equation (1) to calculate the planar Hall resistivity. The calculations are shown in figure 3, which correspond to figure 1 and also show a very good qualitative agreement. The behaviour of the PHE as the direction of the field is reversed is also indicated by the arrows. They agree perfectly with the experimental data in figure 1. A small possible misalignment is also taken into account in the calculation. The result shows that the magnetization reversal in these films can be completely described within a single-domain picture in the light of the SW model. We found this agreement in all the $Fe_{3+x}Si_{1-x}(113)$ films that were studied for composition x between 0.39 and −0.04. The results are summarized in table 1, which shows a summary of different parameters found from the fitting of the PHE data. We also found the same agreement in Fe films of different thicknesses. In figure 4, we show an example of two Fe films with

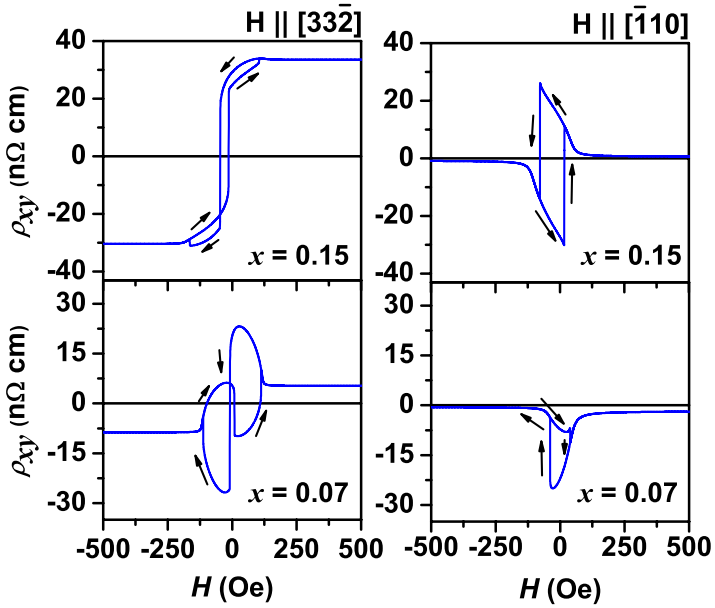

Figure 3. Calculated field dependence of the PHE (ρ_{xy}) from the $Fe_{3+x}Si_{1-x}$ (113) film. The first (second) column is for a magnetic field applied parallel to the major in-plane [33$\bar{2}$] ([$\bar{1}$10]) axis, whereas the first (second) row is for an $Fe_{3+x}Si_{1-x}$ layer with $x = 0.15$ ($x = 0.07$).

Table 1. Summary of data derived by the fitting of planar Hall resistivity of $Fe_{3+x}Si_{1-x}$ and Fe films on GaAs(113)A at 300 K. The magnetic properties such as K_1/M_s and $r = K_u/K_1$ are determined by fitting the low-field behaviour of the PHE. The PHE coefficients ρ^s_{PHE}, ρ^0_{SATM}, and ρ^1_{SATM} are derived by fitting the high-field behaviour of the PHE using equation (1).

Layer	Thickness (nm)	Composition, x	$r = K_u/K_1$	K_1/M_s (Oe)	ρ^s_{PHE} (nΩ cm)	ρ^0_{SATM} (nΩ cm)	ρ^1_{SATM} (nΩ cm)
$Fe_{3+x}Si_{1-x}$	40 ± 1	0.39	0.0	80 ± 5	−9.9	73.8	−14
$Fe_{3+x}Si_{1-x}$	41 ± 1	0.15	−0.3	60 ± 5	−2.7	38	−7
$Fe_{3+x}Si_{1-x}$	42 ± 1	0.07	−0.3	60 ± 5	16.5	16.4	−10
$Fe_{3+x}Si_{1-x}$	46 ± 5	0.05	−0.3	45 ± 5	30.6	2.1	−8.5
$Fe_{3+x}Si_{1-x}$	47 ± 3	0.03	0.0	50 ± 5	21.9	−4.4	−8.7
$Fe_{3+x}Si_{1-x}$	42 ± 5	−0.04	−0.85	50 ± 5	36	−23.5	−8.5
Fe	26	1	0.6	200 ± 20	−9.7	−15.7	8.5
Al/Fe	1.4	1	2.34	135	−7.1	8.2	−3.5

thicknesses of 26 and 1.4 nm. The 1.4 nm Fe film corresponds to only 10 monolayers (ML) of Fe and hence an Al capping layer (20 nm) was grown to prevent oxidation of the layer. The figure shows the angular dependence of the two films with in-plane magnetic fields of $H = +2$ and $+0.5$ kOe. The calculated curves shown as solid lines are obtained by using the SW model for magnetization rotation, as discussed before. Note that the 1.4 nm-thick sample is even reversible, though it is not completely saturated even at $H = +2$ kOe, hence the curve cannot be fitted using equation (1) alone. The best fit is obtained only by calculating ρ_{xy} using the SW model and equation (1), as explained above. The behaviours of the PHE in both films are qualitatively similar. However, the sign and magnitude of the different components are

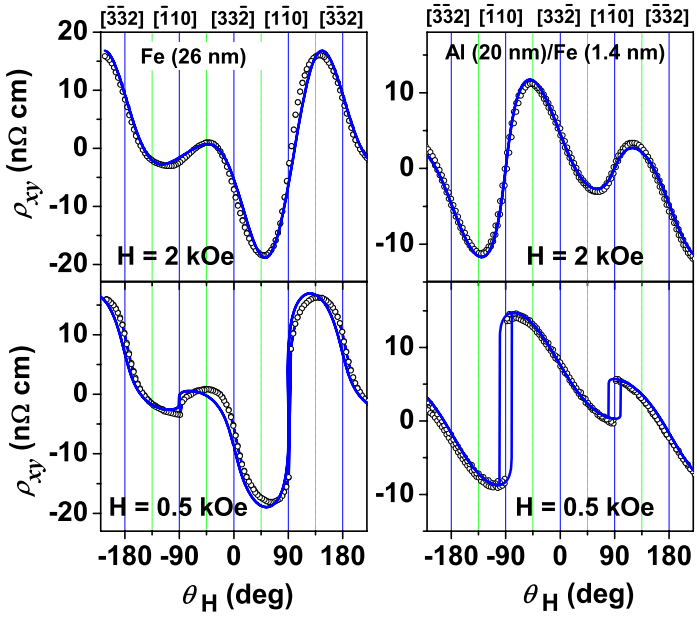

Figure 4. Experimental (symbols) and calculated (thick solid lines) angular dependence of ρ_{xy} (PHE) at magnetic fields of $H = +2$ kOe and $H = +0.5$ kOe for a 26 nm (first column) and a 1.4 nm Fe (second column) film measured at 300 K. Here, $\theta_H = 0°$ indicates the [33$\bar{2}$] direction, which is also the direction of the current. Note that the 1.4 nm Fe film is not completely saturated at $H = +2$ kOe.

different. As shown in figure 4 and table 1, the sign of ρ_{SATM} in the 1.4 nm-thick Fe film is opposite to that of the thicker films. The convention for the sign of ρ_{SATM} is defined in [6]. The opposite sign implies that the interface can play a significant role in determining the sign of the antisymmetric component. It is essential to mention that the PHE measurements of the films shown in figure 4 were performed on rectangular samples with a typical size of 2×4 mm^2. We have also compared the behaviour of the PHE on Hall bar structures with that of the large rectangular samples, in which case a small difference in the switching fields was observed. However, the shape of the PHE was found to be very similar, which indicates that the single-domain model is valid in a wide range of sample dimensions from several μm to several mm^2. The surprising validity of the single-domain model in both $Fe_{3+x}Si_{1-x}$ and Fe films was also observed in SQUID magnetometry [11] and *in situ* magneto-optic Kerr effect experiments [17]. However, consideration of multiple domains should provide more quantitative insight into the observed values of switching fields [18].

4. Discussion

Several interesting phenomena can be deduced from the results summarized in table 1. First, it reports the values of phenomenological coefficients of the PHE for a wide range of compositions of Fe_3Si and different thicknesses of Fe films. Chen *et al* have reported the values of symmetric coefficients for transition metal alloys [19, 20]. However, to our knowledge, the values of the antisymmetric coefficients are never reported in the literature even for the transition metals. The present study involving a low symmetric surface allows us to observe and report these values. It is important to mention that the symmetric amplitude is found to

be different from the anisotropic magnetoresistance. This is a result of the single-crystalline nature of the samples, in agreement with the phenomenological model discussed in [6]. Both the symmetric and antisymmetric coefficients exhibit wide changes in magnitude and sign with composition and thickness of the films. While the actual origin of these phenomena is not clearly understood, this study does provide some insight into the underlying physical origin of the sign changes. For example, stoichiometric Fe_3Si and thick Fe films exhibit the same sign of the saturated antisymmetric transverse resistivity, $\rho_{SATM} = 2(\rho^0_{SATM} + \rho^1_{SATM})$, which is a measure of the antisymmetric component. This implies a relation between the ordering of the Fe_3Si lattice near stoichiometry and the sign of ρ_{SATM}. Besides, the sign of ρ_{SATM} for the 1.4 nm Fe film is reversed compared to the thicker Fe films, which indicates that the interface can also play an important role in thin films in determining the sign of these coefficients. The sign of symmetric coefficients is found to be negative in Fe films and in off-stoichiometric Fe_3Si films. However, a detailed discussion of the physical origin of the sign changes is beyond the scope of this paper.

Table 1 also completely characterizes the magnetic anisotropy of all the samples investigated. In general, we show that the magnetic anisotropy of these samples can be understood by assuming a combination of the four-fold and a uniaxial magnetic anisotropy. The four-fold magnetic anisotropy characterized by the constant K_1, which arises from the magnetocrystalline anisotropy, is a result of the large demagnetization energy of the films [8]. Table 1 shows a positive value of K_1 over the whole composition range, similar to ordered bulk Fe_3Si with $D0_3$ crystal structure [21]. Furthermore, a decrease in K_1/M_s with the addition of Si is also found. Note that, from SQUID magnetometry, we found the saturation magnetization to decrease with the addition of Si [22]. Using the respective saturation magnetization from SQUID magnetometry, this results in $K_1 = (4.6 \pm 1.3) \times 10^5$ erg cm^{-3} for the 26 nm-thick Fe film and $K_1 = (3.0 \pm 0.6) \times 10^4$ erg cm^{-3} for the almost stoichiometric Fe_3Si film. Both values are also comparable to the bulk values of $K_1 = 4.7 \times 10^5$ erg cm^{-3} for bulk Fe and $K_1 = 5.4 \times 10^4$ erg cm^{-3} in ordered Fe_3Si [21]. The decrease in the four-fold magnetic anisotropy constant with increasing Si content can be understood from the argument of the reduced symmetry environment of the Fe atoms in the crystal lattice due to the addition of Si. Since the magnetocrystalline anisotropy arises from the spin–orbit coupling, the decrease in K_1 implies a decrease in spin–orbit coupling strength with the addition of Si.

The ratio r, which reflects the strength of the additional UMA, also exhibits several interesting phenomena. First, it is positive for Fe films, which implies an easy axis along $[33\bar{2}]$ and is found to increase with decreasing thickness, in perfect agreement with the results of SQUID magnetometry [8, 11] and anisotropic magnetoresistance [3]. As explained in [8, 11], the UMA in these Fe films is an interfacial effect and is determined by the anisotropic bonding structure at the interface. However, in Fe_3Si films, the ratio r is negative and increases in amplitude with increasing Si content (decreasing x)—with the exception of one sample with $x = 0.03$. The negative sign of r, which indicates an easy axis of the UMA along the $[\bar{1}10]$ direction, is opposite to that of the above interface-related UMA in the Fe films of [8, 11]. Hence, the UMA observed here is probably not related to the interface. Besides, the thickness range (40–50 nm) studied here may be substantially too large to observe any interface-related effect. However, for $Fe_3Si(001)$ films in this thickness range, a UMA [23, 24] of interfacial origin [25] has recently been reported. For this reason, the role of the interface should not be discarded so easily. A detailed thickness dependence study is required to confirm the role of the interface on the negative r observed in these [113]-oriented films. The surface morphology of these films does not exhibit any anisotropic roughness, thus ruling out a surface-morphology-related dipolar origin of the UMA. The other possible origin of the UMA includes the growth conditions, the presence of some additional phase, and the strain in the films. To investigate

the influence of the former, we have also studied the growth temperature dependence for the stoichiometric $Fe_{3+x}Si_{1-x}$ sample $x = 0.03$ with SQUID magnetometry. However, from these studies we only witness an increase in the coercive field H_c with $r = 0$, remaining constant when the growth temperature is increased above 250 °C. The increase in H_c is essentially due to the degradation of the layer quality. However, the preservation of $r = 0$ indicates that the four-fold magnetic anisotropy is dominant in this growth temperature range. This shows that the growth conditions do not have a significant influence on this UMA, at least in the temperature range studied. A strong UMA is actually observed for samples with high Si content (e.g. $x = -0.04$), for which the presence of some additional phase is also known from reflection high-energy electron diffraction and high-resolution x-ray diffraction experiments [7]. However, the composition of this possible phase and its relation to the UMA are not known clearly. Thus the UMA observed here is not completely understood. However, these studies indicate that it might be related to interfacial bonding like that of Fe films or some interfacial reactions at the interface. Note that strain is an unlikely origin of this UMA, since the lattice mismatch between Fe_3Si and GaAs is much smaller compared to the Fe/GaAs system, for which the UMA is known to be strain independent [26]. Besides, all the Fe_3Si films that were studied were found to be coherent, and hence no in-plane anisotropic strain is supposed to be present in these films.

5. Conclusion

In conclusion, we report an extensive study of the planar Hall effect in Fe_3Si and Fe films grown on low-symmetry GaAs(113)A substrates over a range of compositions and several thicknesses. The result of this study is two-fold. First, it completely characterizes the magnetic anisotropic properties of the films using the planar Hall effect as a tool and identifies the simple Stoner–Wolfarth model as a qualitative description for the magnetization reversal. This is possible despite the presence of the antisymmetric component in the PHE, which complicates the behaviour and the shape of the planar Hall effect. Second, the study reports the phenomenological symmetric and antisymmetric coefficients and their behaviour with the composition and thickness of the films.

Acknowledgments

The authors would like to thank E Wiebicke and A Riedel for Hall bar sample preparation. We would also like to thank M Bowen, L Däweritz, R Hey, and B Jenichen for useful discussions. Part of this work has been founded by the German Bundesministerium für Bildung und Forschung under the research program *NanoQuit* (contract no. 01BM463).

References

[1] Tang H X, Kawakami R K, Awschalom D D and Roukes M L 2003 *Phys. Rev. Lett.* **90** 107201
[2] Kreutz T C, Allen W D, Gwinn E G, Awschalom D D and Gossard A C 2004 *Phys. Rev.* B **69** 081302
[3] Friedland K J, Herfort J, Muduli P K, Schönherr H P and Ploog K H 2005 *J. Supercond.* **18** 309
[4] Wang K Y, Edmonds K W, Campion R P, Zhao L X, Foxon C T and Gallagher B L 2005 *Phys. Rev.* B **72** 085201
[5] Friedland K J, Nötzel R, Schönherr H P, Riedel A, Kostial H and Ploog K 2001 *Physica* E **10** 442
[6] Muduli P K, Friedland K J, Herfort J, Schönherr H P and Ploog K H 2005 *Phys. Rev.* B **72** 104430
[7] Muduli P K, Herfort J, Schönherr H P and Ploog K H 2005 *J. Cryst. Growth* **285** 508
[8] Muduli P K, Herfort J, Schönherr H P and Ploog K H 2005 *J. Appl. Phys.* **97** 3904
[9] Hansen M 1958 *Constitution of Binary Alloys* (New York: McGraw-Hill)
[10] Elliot R P 1965 *Constitution of Binary Alloys, Suppl. 1* (New York: McGraw-Hill)

[11] Muduli P K, Herfort J, Schönherr H P, Däweritz L and Ploog K H 2005 *Appl. Phys.* A **81** 901
[12] Gester M, Daboo C, Hicken R J, Gray S J, Ercole A and Bland J A C 1996 *J. Appl. Phys.* **80** 347
[13] Florczak J M and Dahlberg E D 1991 *Phys. Rev.* B **44** 9338
[14] Gu E, Bland J A C, Daboo C, Gester M, Brown L M, Ploessl R and Chapman J N 1995 *Phys. Rev.* B **51** 3596
[15] Riggs K T, Dahlberg E D and Prinz G A 1990 *Phys. Rev.* B **41** 7088
[16] Stoner E C and Wohlfarth E P 1948 *Phil. Trans. R. Soc.* A **240** 74
[17] Muduli P K 2006 *PhD Thesis* Humboldt University, Berlin http://edoc.hu-berlin.de/docviews/abstract.php?id=27224
[18] Daboo C, Hicken R J, Gu E, Gester M, Gray S J, Eley D E P, Ahmad E, Bland J A C, Ploessl R and Chapman J N 1995 *Phys. Rev.* B **51** 15964
[19] Chen T T and Marsocci V A 1972 *Physica* **59** 498
[20] Chen T T and Marsocci V A 1972 *Solid State Commun.* **10** 783
[21] Goto M and Kamimori T 1983 *J. Phys. Soc. Japan* **52** 3710
[22] Herfort J, Muduli P K, Friedland K J, Schönherr H P and Ploog K H 2006 *J. Magn. Magn. Mater.* at press
[23] Herfort J, Schönherr H P, Friedland K J and Ploog K H 2004 *J. Vac. Sci. Technol.* B **22** 2073
[24] Ionescu A, Vaz C A F, Trypiniotis T, Gurtler C M, Garcia-Miquel H, Bland J A C, Vickers M E, Dalgliesh R M, Langridge S, Bugoslavsky Y, Miyoshi Y, Cohen L F and Ziebeck K R A 2005 *Phys. Rev.* B **71** 094401
[25] Lenz K, Kosubek E, Baberschke K, Wende H, Herfort J, Schönherr H P and Ploog K H 2005 *Phys. Rev.* B **72** 144411
[26] Thomas O, Shen Q, Schieffer P, Tournerie N and Lépine B 2003 *Phys. Rev. Lett.* **90** 017205